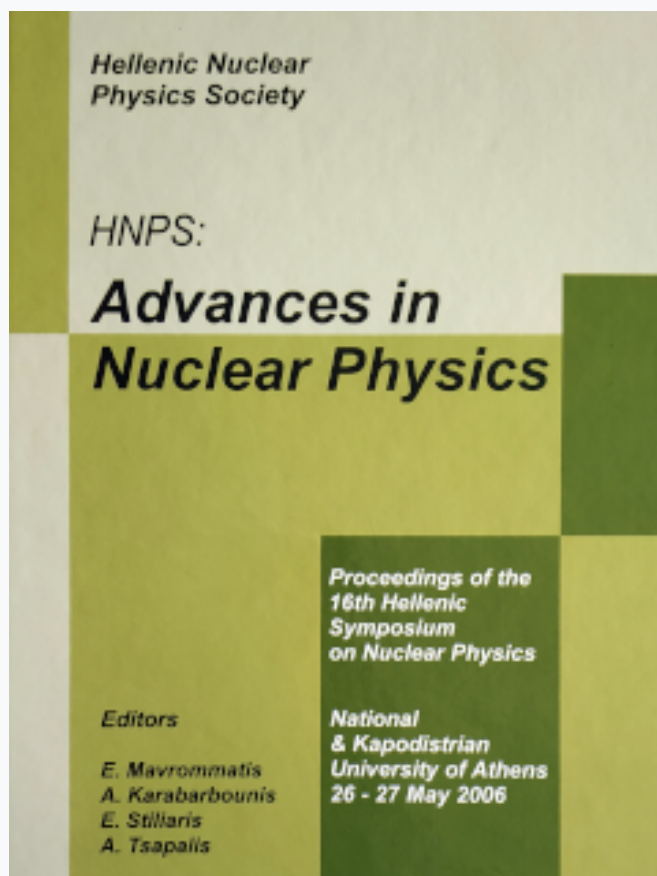


## HNPS Advances in Nuclear Physics

Vol 15 (2006)

HNPS2006



### A $4\pi$ $\gamma$ -summing method for cross-section measurements of capture reactions

A. Spyrou, H.-W. Becker, A. Lagoyannis, S. Harissopulos, C. Rolfs

doi: [10.12681/hnps.2627](https://doi.org/10.12681/hnps.2627)

#### To cite this article:

Spyrou, A., Becker, H.-W., Lagoyannis, A., Harissopulos, S., & Rolfs, C. (2020). A  $4\pi$   $\gamma$ -summing method for cross-section measurements of capture reactions. *HNPS Advances in Nuclear Physics*, 15, 111–117.

<https://doi.org/10.12681/hnps.2627>

## A $4\pi$ $\gamma$ -summing method for cross-section measurements of capture reactions.

A. Spyrou<sup>a</sup>, H.-W. Becker<sup>b</sup>, A. Lagoyannis<sup>a</sup>, S. Harissopulos<sup>a</sup>, C. Rolfs<sup>b</sup>.

<sup>a</sup>Institute of Nuclear Physics, National Center for Scientific Research “Demokritos”, POB 60228, 153.10 Aghia Paraskevi, Athens, Greece.

<sup>b</sup>DTL, Institut für Experimentalphysik III, Ruhr-Universität Bochum, Universitätsstr. 150, 40781 Bochum, Germany.

Capture reaction cross sections at energies far below the Coulomb barrier are of major importance for the understanding of stellar nucleosynthesis. Since the cross sections of the majority of these reactions are very small, the use of high efficiency detectors is essential. In this work, a new method for capture reaction cross section measurements based on a large volume  $4\pi$  NaI detector is presented.

### 1. Introduction

The understanding of stellar nucleosynthesis processes often requires the knowledge of the cross sections of several thousands of nuclear reactions, the majority of which are capture reactions with very low cross sections. As the latter lie in the  $\mu$ barn regime or even below their determination is not always an easy task. This task is realized by employing the activation technique [1], measuring  $\gamma$ -angular distributions [2] or, alternatively angle-integrated  $\gamma$  fluxes. In the present work we used the latter method to carry out systematic cross section measurements of proton and  $\alpha$ -particle capture reactions on medium-heavy nuclei.

The working principle of the method employed relies on a) the long time response and b) the large volume of a  $12\times 12$  inch NaI detector with a bore hole along its axis. The large volume of this detector enables to fully absorb the photons emitted by the reaction of interest, while the long time response results in the summation of these photons when emitted within a time shorter than  $\simeq 250$  ns. The working principle is illustrated in Fig. 1. In Fig. 1b one finds the  $\gamma$  spectrum that is expected with a small size NaI detector from the de-excitation of the compound nucleus, which is produced in the simple case of the capture reaction shown in part a) of Fig. 1. According to the level scheme of Fig. 1a the produced nucleus de-excites from its entry state by emitting  $\gamma$  rays that feed directly the ground state ( $\gamma_0$  transition), or form  $\gamma$  cascades (successive  $\gamma$  rays between different excited states). As shown in part b), the spectrum expected for a small size NaI detector includes all peaks corresponding to the  $\gamma$  transitions shown in the level scheme together with the accompanying Compton continuum. In the case, however, of a large volume NaI detector (part c) the  $\gamma$  spectrum expected is completely different, i.e. it consists of just

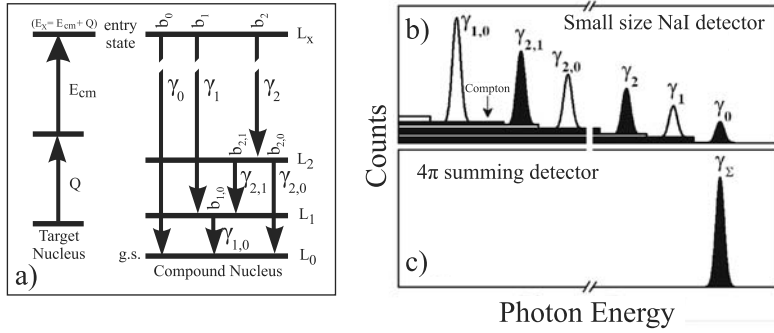


Figure 1. Typical  $\gamma$  spectra expected for the capture reaction shown in part a). Spectra shown in b) and c) correspond to a small size and a large volume  $4\pi$  NaI detector, respectively.

one peak, called *sum peak*, resulting from the summation of sequential photons in a  $\gamma$  cascade. For the case of the simple level scheme shown in Fig. 1a, there exist four different cascades, which contribute to the sum peak. These are: 1)  $\gamma_1 \rightarrow \gamma_{1,0}$ , 2)  $\gamma_2 \rightarrow \gamma_{2,0}$ , 3)  $\gamma_2 \rightarrow \gamma_{2,1} \rightarrow \gamma_{1,0}$ , and 4)  $\gamma_0$ . As a result, the intensity of the sum peak corresponds to the total number of photons de-exciting the entry state. Hence, the area  $A_\Sigma$  of the sum peak can be used to determine the cross section from

$$\sigma = \frac{A_t}{N_A \xi_t} \frac{1}{N_b} \frac{A_\Sigma}{\varepsilon_\Sigma} \quad (1)$$

where,  $A_t$  and  $\xi_t$  are the mass number of the target and its thickness, respectively,  $N_A$  is the Avogadro number,  $N_b$  is the number of beam particles and  $\varepsilon_\Sigma$  is the sum-peak efficiency.

According to Eq. 1 one needs to acquire only one spectrum and analyze only one peak, i.e. the sum peak, in order to determine the cross section of interest. However, the main problem in applying Eq. 1 is the sum-peak efficiency  $\varepsilon_\Sigma$ : This depends strongly on the multiplicity  $M$  of the  $\gamma$  cascades de-exciting the entry state that, in most cases, is unknown. This problem motivated us to develop a method to, first, determine the multiplicity and then the corresponding sum-peak efficiency. The setup used in the present work is presented in section 2. In section 3, we introduce a new method, in the following called “in/out ratio method” that allows to determine multiplicities. Section 4 refers to the determination of the sum-peak efficiency. The measurements performed are finally presented in section 5.

## 2. The experimental setup

The measurements of the present work were carried out at the Dynamitron Tandem Laboratorium (DTL) of the University of Bochum, Germany. As shown in Fig. 2, the setup consisted of a  $12 \times 12$  inch NaI(Tl) detector (BICRON) with a bore hole ( $\varnothing$  35 mm) along its axis. The detector had an energy resolution of  $\simeq 2\%$  at a photon energy of  $\simeq 10$  MeV and covered a solid angle of almost 98% of  $4\pi$  for photons emitted at its center. Six

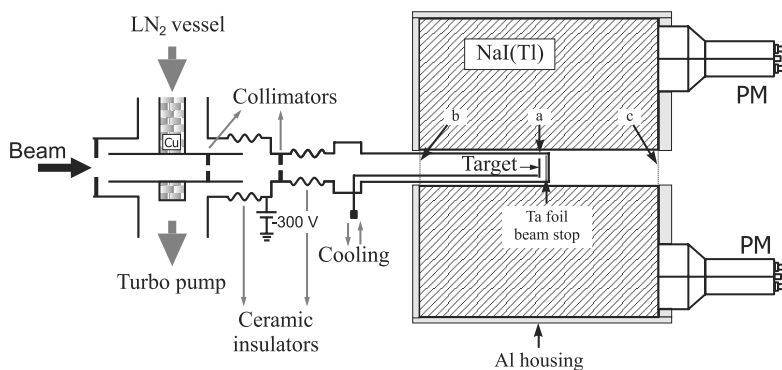


Figure 2. Layout of the experimental setup used in the present work.

photomultipliers (PM) were accumulating the fluorescence light and the resulting signals were gain matched by appropriate high-voltage settings and then summed. The final summed signal was fed into a spectroscopy amplifier and the exit signal was guided to the Multi-Channel Analyzer (MCA).

As shown in Fig. 2, the beam axis was defined by two Ta apertures, resulting to a beam spot of  $\approx 2$  mm in diameter. Both apertures, as well as the beam line, were electrically isolated to optimize the ion-beam focussing. A voltage of -300 V was applied, as shown in Fig. 2, to suppress secondary electrons. The beam was stopped at the end of the tube by using a thick Ta foil. The vacuum was kept at  $\approx 1 \times 10^{-7}$  mbar by means of a turbo molecular pump combined with a cool trap. As a result, no carbon built-up was observed on the targets. The latter were mounted on a Ta holder that was placed at the center of the bore hole of the detector. The targets were cooled with air flowing in a stainless steel pipe ( $\varnothing 3$  mm), which surrounded the target holder.

### 3. The in/out ratio method

As mentioned in section 1, the sum-peak efficiency depends not only on the energy of the sum peak but also on the multiplicity  $M$  of the cascading  $\gamma$  transitions that give rise to the sum peak. In this section we present the “in/out-ratio” method, which allows to determine the unknown multiplicity of the summed  $\gamma$  cascades. To illustrate the method let us assume that a single  $\gamma$  ray is emitted at the center of the NaI detector, i.e. at position “a” of Fig. 2 resulting to a peak in the spectrum having an intensity  $I^{in}$ . Obviously, the same  $\gamma$  ray, when emitted at the edge of the detector (positions “b” or “c” of Fig. 2), results to a peak with an intensity  $I^{out} = I^{in}/2$ . This is because the solid angle covered by the detector is decreased to 50%. If we further assume that a  $\gamma$  cascade of multiplicity  $M=2$  is emitted at positions “a” and “b” or “c” of Fig. 2 then the ratio  $R = I^{in}/I^{out}$  will be  $R = 2 \times 2 = 4$ . Furthermore, this ratio will be  $R = 2 \times 2 \times 2 = 8$  and  $R = 2 \times 2 \times 2 \times 2 = 16$  for  $\gamma$  cascades with multiplicities  $M=3$  and  $M=4$ , respectively. Under these conditions, a ratio  $R = 2^M$  is ideally expected for a cascade of multiplicity  $M$ .

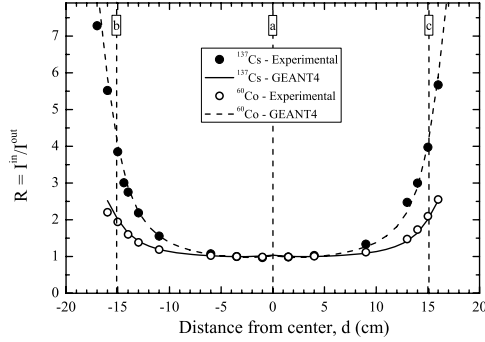


Figure 3. In/out ratio  $R$  obtained with a  $^{137}\text{Cs}$  source (open circles) and a  $^{60}\text{Co}$  source (black dots) at various distances from the center of the detector along the bore hole axis. The solid curves are the result of the corresponding GEANT4 simulations.

In the present work, we first tested the in/out ratio method by means of two standard calibrating  $\gamma$  sources of well known activities, i.e.  $^{137}\text{Cs}$  and  $^{60}\text{Co}$ . In the case of  $^{137}\text{Cs}$  a single  $\gamma$  ray ( $M=1$ ) is emitted while in the case of  $^{60}\text{Co}$  the emitted  $\gamma$  transitions form a pure (99.9%)  $M=2$  cascade.  $^{137}\text{Cs}$ - and  $^{60}\text{Co}$ -source spectra were respectively accumulated at 15 and 17 different positions along the bore hole of the detector. From these spectra we were able to obtain the in/out ratio  $R = I^{in}/I^{out}$ . The results are shown in Fig. 3. Hereby, the open circles and the black dots correspond to the ratios  $R$  measured with  $^{137}\text{Cs}$  and  $^{60}\text{Co}$ , respectively. In the same figure one can see that at the two detector edges, i.e. at positions “b” and “c” having a distance of  $\pm 15.3$  cm from the center of the detector, one reads  $R=2$  and 4 for  $^{137}\text{Cs}$  and  $^{60}\text{Co}$ , respectively. Both values are in excellent agreement with the expected ones. The solid lines shown in Fig. 3 are the corresponding GEANT4 simulations.

After having successfully checked the validity of the basic idea of the in/out ratio method with pure  $M=1$  and  $M=2$  cascades, our next step was to use cases where compound nuclei de-excite via multiple cascades of different multiplicities. For this purpose, resonant capture reactions with well known branchings and strengths were used. In this type of reactions, however, the  $\gamma$  cascades yielding the sum peak may have different multiplicities. Therefore, one deals with an average multiplicity  $\langle M \rangle$  and the ratio  $R$  has to be expressed as  $R = \alpha^{\langle M \rangle}$ , with  $\alpha = 2$ , when  $R$  is determined at the edge of the NaI crystal. The average multiplicity  $\langle M \rangle$  is defined as:

$$\langle M \rangle = \sum_i B_i M_i \quad (2)$$

where  $M_i$  is the multiplicity of the  $i$ -th  $\gamma$  cascade and  $B_i$  is the product of the  $\gamma$  branchings of the transitions participating in the  $i$ -th cascade.

The resonances used to derive the empirical relation  $R = \alpha^{\langle M \rangle}$  are given in Tab. 1 together with the thickness  $\xi$  of the targets used, the relevant resonance strengths  $\omega\gamma$ , the corresponding sum-peak energies  $E_\Sigma$  and the average multiplicities  $\langle M \rangle$ . The latter

Table 1

Resonances used to determine the sum-peak efficiency of the  $4\pi$  summing detector. The experimentally determined sum-peak efficiency  $\varepsilon_{\Sigma}^{exp}$  and the corresponding GEANT4-simulated one  $\varepsilon_{\Sigma}^{sim}$  are given in the 7th and 8th column, respectively.

eac. i n	$(g \text{ cm}^2)$	$R$ ( e )	( e )	$\Sigma$ ( e )	$\varepsilon_{\Sigma}^{exp}$	$\varepsilon_{\Sigma}^{sim}$
26 g(p, ) <sup>27</sup> l	$\pm$		. $\pm$ . $\text{---}$	. $\text{---}$	. $\pm$ .	.
			. $\pm$ . $\text{---}$	. $\text{---}$	. $\pm$ .	.
			. $\pm$ . $\text{---}$	. $\text{---}$	. $\pm$ .	.
			. $\pm$ . $\text{---}$	. $\text{---}$	. $\pm$ .	.
			. $\pm$ . $\text{---}$	. $\text{---}$	. $\pm$ .	.
27 l(p, ) <sup>28</sup> i	$\pm$		. $\pm$ . $\text{---}$	. $\text{---}$	. $\pm$ .	.
			. $\pm$ . $\text{---}$	. $\text{---}$	. $\pm$ .	.
			. $\pm$ . $\text{---}$	. $\text{---}$	. $\pm$ .	.
28 i( ) <sup>32</sup>	$\pm$		. $\pm$ . $\text{---}$	. $\text{---}$	. $\pm$ .	.

quantities have been calculated using Eq. 2. The relevant branchings were taken from the literature. For all resonances of Tab. 1, we determined in/out ratios at a distance  $d=16.8$  cm. This distance was longer than that of position “b” (see Fig. 2) and kept fixed for all measurements. The obtained  $R$  values vs.  $\langle M \rangle$  are shown in Fig. 4a) together with those obtained with  $^{137}\text{Cs}$  and  $^{60}\text{Co}$  at the same distance. By fitting the data of Fig. 4a (solid curve) we obtained:

$$R = 2.48(3)^{\langle M \rangle} \quad (3)$$

This equation was used to obtain the average multiplicity  $\langle M \rangle$  of the capture reactions investigated from the ratios  $R$  measured. Once  $\langle M \rangle$  was obtained, we were able to derive the corresponding sum-peak efficiency  $\varepsilon_{\Sigma}$  as described in the following section.

#### 4. Sum-peak efficiency

In order to determine the sum-peak efficiency  $\varepsilon_{\Sigma}$  of our summing detector we used the Monte Carlo code GEANT4 [7] to simulate spectra resulting from the decay of compound nuclei that are de-excited via  $\gamma$  cascades of various multiplicities  $M$  yielding sum peaks of energies between 8 and 16 MeV. In our simulations the geometry of the setup was properly described by means of 10 different volumes. The results obtained for  $M=1$  to 7 are shown as curves in Fig. 4b. On the other hand, we used the resonances given in Tab. 1 to determine experimentally the efficiency of the corresponding sum peaks. This task was performed by measuring  $\gamma$  spectra at the plateau of these resonances and further determining  $\varepsilon_{\Sigma}$  from the corresponding sum-peak intensities  $I_{\Sigma}$  using:

$$\omega\gamma = \frac{1}{\varepsilon_{\Sigma}} \frac{I_{\Sigma}}{N_b} \frac{2}{\lambda^2} \frac{A}{N_A} \frac{M}{M+m} T(E) \quad (4)$$

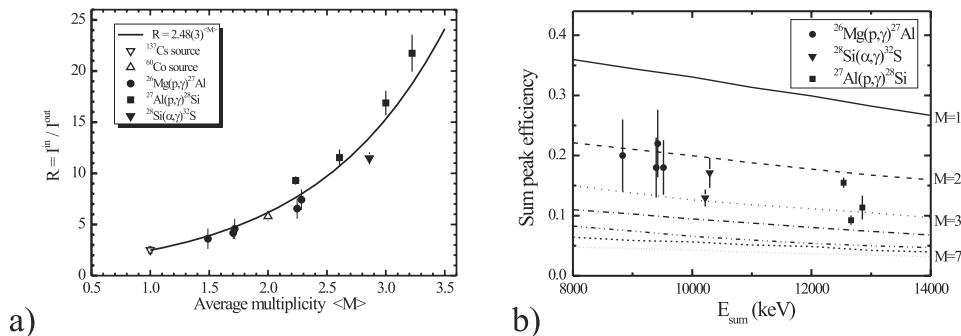


Figure 4. a) Plot of the in/out ratio of the resonances presented in Tab. 1 as a function of their average multiplicities. b) Plot of the efficiency of the summing NaI detector as a function of the energy of the sum-peak. The different curves correspond to simulations of sum peaks of different multiplicities ( $M=1$  to  $7$ ), while the data points represent experimental results for the resonances of Tab. 1.

where  $N_b$  is the number of the beam particles,  $A$  is the atomic weight of the target,  $N_A$  is the Avogadro number,  $m$  and  $M$  are the beam and target masses, respectively,  $\lambda$  is the incident beam wavelength and  $T(E)$  is the stopping power of the beam in the target. The results,  $\varepsilon_{\Sigma}^{\text{exp}}$  are given in Tab. 1 together with the corresponding simulated ones,  $\varepsilon_{\Sigma}^{\text{sim}}$ . As it can be seen, the agreement is very good. In addition, from the “position” of the  $\varepsilon_{\Sigma}^{\text{exp}}$  data points in Fig. 4b, it becomes clear that the sum-peak efficiency resulted from our GEANT4 simulations for various multiplicities  $M$  is very reliable (compare the corresponding  $\langle M \rangle$  in Tab. 1). This allowed us to adopt the sum-peak efficiency curves plotted in Fig. 4b to apply Eq. 1 depending on the average multiplicity  $\langle M \rangle$  of the reaction of interest. The latter quantity was obtained from the experimentally determined in/out ratio  $R$  using Eq. 3.

## 5. Cross section measurements

In order to test the reliability of our method we performed cross section measurements of the  $^{62}\text{Ni}(\alpha, \gamma)^{66}\text{Zn}$  reaction, which has a very well known cross section [8]. Our measurements were carried out using a 98%-enriched self-supporting  $^{62}\text{Ni}$  target, with  $413 \pm 29 \mu\text{g}/\text{cm}^2$  thickness. The  $\alpha$ -beam current on target was ranging between 6 and 140 nA. In/out ratios were measured at 10 different  $\alpha$ -beam energies between 5 and 9 MeV. From these ratios, we obtained average multiplicities  $\langle M \rangle$  using Eq. 3. Based on the  $\langle M \rangle$  values, the corresponding sum-peak efficiency curve of Fig. 4b was then adopted to further apply Eq. 1.

The results of our work (black dots) are compared to the data (open circles) of Zyskind *et al.* [8] in Fig. 5. As shown in this figure the agreement is excellent. This implies that our method is reliable and can, therefore, be used to study capture reactions of astrophysical interest.

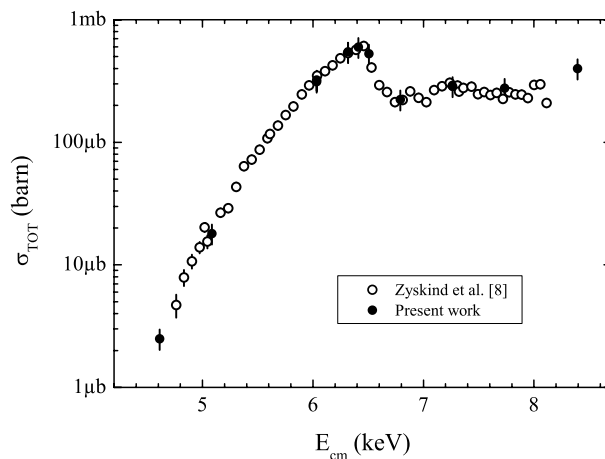


Figure 5. Cross section measurements of the  $^{62}\text{Ni}(\alpha, \gamma)^{66}\text{Zn}$  reaction. The black dots represent the results of the present work while the open circles correspond to the results of the previous work of Zyskind *et al.* [8].

### Acknowledgments

This work was supported by the Hellenic State Scholarship Foundation (IKY), the German Academic Exchange Service (DAAD), and the Dynamitron - Tandem - Laboratorium (DTL) of the University of Bochum.

### REFERENCES

1. T. Sauter and F. Käppeler, *Phys. Rev. C* **55** (1997) 3127.
2. S. Galanopoulos *et al.* *Phys. Rev.* **C67**, 015801 (2003).
3. J. J. A. Smit, J.P.L. Reinecke, M.A. Meyer, D. Reitmann, and P.M. Endt, *Nucl. Phys.* **A377**, (1982) 15.
4. C. Chronidou, K. Spyrou, S. Harissopoulos, S. Kossionides, T. Paradellis, *Eur. Phys. J* **A6**, (1999) 303.
5. M. A. Meyer, I. Venter, and D. Reitmann, *Nucl. Phys.* **A250** (1975) 235.
6. D. W. O. Rogers, W. R. Dixon and R. S. Storey, *Nucl. Phys.* **A281**, (1977) 345.
7. GEANT4: A simulation Toolkit, S. Agostnelli *et al.*, *Nucl. Instr. Meth.* **A506** (2003) 250.
8. J. L. Zyskind, J. M. Davidson, M. T. Esat, M. H. Shapiro and R. H. Spear, *Nucl. Phys.* **A331**, (1979) 180.